Gold Bull (2014) 47:47–55
DOI 10.1007/s13404-013-0111-z

ORIGINAL PAPER

The effect of nonhomogeneous silver coating on the plasmonic absorption of Au–Ag core–shell nanorod

Jian Zhu · Fan Zhang · Jian-Jun Li · Jun-Wu Zhao

Published online: 4 October 2013

Abstract Plasmonic light absorption properties of bimetallic Au–Ag core–shell nanorod with nonhomogeneous Ag coating are investigated both theoretically and experimentally. When the Ag coating on the Au nanorod is not homogeneous, the overall aspect ratio and Ag composition greatly depends on the coating uniform, which strongly affects intensity changing and wavelength shift of the plasmonic absorption. When the transverse Ag coating is faster than longitudinal coating, the Au–Ag core–shell nanorod could present two intense longitudinal plasmonic absorption peaks with equal intensity and small wavelength gap as the Ag shell thickness has a critical value. Furthermore, this critical Ag shell thickness could be decreased when the Au nanorod core has a small aspect ratio. When the longitudinal Ag coating is faster than transverse coating, the increasing intensity of longitudinal peak corresponding to outer Ag surface is always weaker than the longitudinal peak corresponding to Au–Ag interface. Thus, we cannot obtain two equal intense plasmonic absorption peaks when the longitudinal Ag coating is thicker than the transverse coating. However, the transverse peak corresponding to Au–Ag interface could be enhanced by decreasing the aspect ratio of the Au nanorod core. Thus, we can always find three distinct absorption peaks as the aspect ratio of Au nanorod is decreased and the longitudinal Ag coating is greater than transverse coating.

Keywords Au–Ag bimetallic nanoparticles · Nonhomogeneous silver coating · Core–shell structure · Nanorod · Plasmonic absorption

J. Zhu (✉) · F. Zhang · J.-J. Li · J.-W. Zhao (✉)
The Key Laboratory of Biomedical Information Engineering of Ministry of Education, School of Life Science and Technology, Xi'an Jiaotong University, Xi'an, 710049, People's Republic of China
e-mail: jianzhusummer@163.com
e-mail: nanoptzhao@163.com

Introduction

In recent years, noble metallic nanoparticles have received considerable attention owing to their novel optical properties based on localized surface plasmon resonance (LSPR). Although noble metal gold and silver have the same face-centered cubic crystal structure and similar lattice constants, silver nanoparticles display stronger LSPR absorption with higher plasmon energy (about 400 nm for Ag nanosphere and 520 nm for Au nanosphere) and more intense local electric field enhancement [1–3]. Therefore, Ag nanoparticles have been often used as substrates for surface-enhanced Raman scattering (SERS) [4] and sensing and imaging based on resonance light scattering [5, 6].

Because symmetry breaking induced redistribution of surface charges, the plasmonic optical properties are strongly dependent on particle shape. Thus, producing metallic nanoparticles with low symmetry (nonspherical symmetry) could improve plasmon tunability such as resonance wavelength and local field intensity [7, 8]. However, the synthesis of complex morphological silver nanoparticles such as Ag nanorod is much harder than gold [9]. One of the effective methods to achieve nanoparticles with well-defined morphology and silver surface is coating an Ag nanolayer on the premade gold nanoparticles with nonspherical symmetry [9–12].

By using the microwave-polyol method, Au–Ag core–shell nanocrystals have been successfully synthesized [10]. The corresponding crystal structures and their growth mechanisms had also been studied. Furthermore, the transmission electron microscope (TEM) images observed by Tsuji et al. demonstrated that the shapes of initiated Au seeds greatly affect the shapes of formed Ag shells [13]. The Au–Ag core–shell nanocubes with varying shaped cores have been reported by Gong et al. [14]. The prepared Au–Ag core–shell nanoparticles display very abundant and distinct LSPR

characteristics, which are dependent on core shape and core size. By using iodide ions, the growth direction of the Ag shell on the gold nanodisk core could also be tuned, and then the shape of the coated Ag shell could also be controlled [15]. The LSPR and SERS response in Au dumb bells with silver coating have also been reported [9]; this type of core–shell Au–Ag nanostructure is expected to serve as excellent SERS substrates because of the higher enhancement factors for silver as compared to gold. Ma et al. reported a facile method for generating Au–Ag core–shell nanocubes with controllable edge lengths [16]. By varying the ratio of Ag ions to Au seeds, the thickness of the Ag shells could be finely tuned from 1.2 to 20 nm, and the plasmon excitation of the Au cores would be completely screened when the Ag shell has a critical value of 3 nm. The refractive index sensitivity of gold–silver core–shell nanoparticles has also been studied [17]. It has been found that coating a layer of silver brings about a higher refractive index sensitivity in comparison to the pure Au nanobars [18].

It is known that the Ag and Au nanorods have two LSPR bands corresponding to transverse and longitudinal resonance, respectively. The longitudinal plasmon bands are sensitive to the aspect ratio and could be tuned from visible to infrared region. An interesting topic arises from the effect of Ag coating on the LSPR of Au–Ag core–shell nanorods. In our previous theoretical study, two transverse LSPR bands from outer Ag surface and Au–Ag interface have been observed in Au–Ag core–shell nanowires [19]. In the report of Yu et al. [20], the optical properties of bimetallic Au–Ag core–shell nanorods were characterized by using a steady-state extinction spectra and ultrafast transient absorption spectroscopy. They have experimentally observed two longitudinal LSPR bands in Au–Ag core–shell nanorods corresponding to the Ag shell and Au core. In the study of Liu et al., the silver coating induced blue shift, and enhancement of longitudinal plasmon mode was observed [21]. And the blue shift has been attributed to the changing of effective dielectric function and decreasing of the overall aspect ratio induced by silver coating.

In a recent report, it is interesting to find that the silver coating is not always homogeneous [3]. In the preparation method of Jiang et al., the thickness of the Ag shell at the side increases faster than that at the ends as the amounts of $AgNO_3$ is increased [3]. How about the effect of nonhomogeneous silver coating on the plasmonic absorption properties of gold nanorod? In this report, we studied the plasmonic absorption properties of Au–Ag core–shell nanostructure with nonhomogeneous Ag coating. It has been found that the anisotropy of Ag coating greatly affects intensity changing, wavelength shift, and peak number of the plasmonic absorption. Furthermore, the physical origin of the nonhomogeneous Ag coating-dependent LSPR tunability has also been discussed.

The model

The geometry of the core–shell structure Au–Ag ellipsoidal nanorods with rotation symmetry is shown in Fig. 1. The Au ellipsoid core is modeled as a prolate (cigar shaped) spheroid, which is generated by rotating an ellipse about its major axis. Because of the rotation symmetry, the Au ellipsoid core has a semimajor axis c_1 and equal semiminor axis $a_1=b_1$. The outer surface of the Ag shell has semimajor axis c_2 and semiminor axis $a_2=b_2$. And the coated Ag shell has a transverse thickness of $t_T=a_2-a_1$ and longitudinal thickness of $t_L=c_2-c_1$. When the silver is homogeneously coated on the gold nanorod, t_T and t_L have the same value. In this model, the dielectric constant of the Au nanorod core, Ag coating shell, and environmental medium is given by ε_1, ε_2, and ε_3, respectively. It is important to note that the dielectric function ε_1 and ε_2 have real and imaginary wavelength (λ)-dependent components [22]. In our analysis, the size of the Au–Ag nanostructure is much smaller than the incident wavelength. Thus, the nanoparticles are subjected to an almost uniform field and oscillate like a simple dipole. Therefore, the quasistatic approximation can be employed in the calculation. The basic equations of the polarizabilities along the principal axes and the plasmonic absorption cross-sections could be derived from the Laplace's equation and have been reported in [21, 23]. By plotting the absorption cross-sections with different wavelength, we could obtain the absorption spectrum.

Results and discussion

Absorption spectra of Au–Ag nanorods with homogeneous silver coating

Figure 2a shows the calculated absorption spectra of bare Au nanorods and Au–Ag core–shell nanorods with homogeneous Ag coating. In this calculation, the semiminor axis of the inner Au nanorod is set as a_1= 5 nm, the aspect ratios of the Au nanorod is set as $p=c_1/a_1=4$, the environmental dielectric constant is set as $\varepsilon_3=1.0$. For pure Au nanorods, there are two LSPR absorption peaks corresponding to transverse and longitudinal resonance appearing at about 515 and 686 nm, respectively. As the coating Ag shell thickness is increased from 1 to 11 nm, both the transverse (denoted as peak 2) and longitudinal (denoted as peak 3) peaks blue shift and get intense. However, the shifting and intensity increase of the longitudinal peak are more intense, and then peak 2 has been merged gradually by peak 3. What is more, the Ag coating results in a new plasmonic absorption peak taking place at shorter wavelength, which is denoted as peak 1. As the coating Ag shell thickness is increased, the peak 1 red shifts slightly and gets intense greatly. All these Ag coating-dependent absorption properties are in good agreement with the

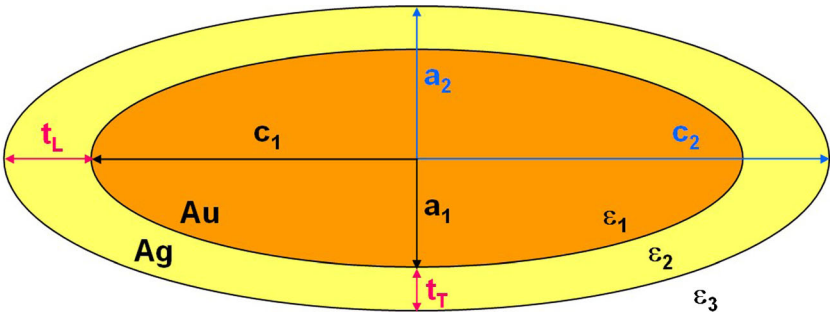

Fig. 1 Geometry of core–shell structure Au–Ag ellipsoidal nanorods: ε_1, ε_2, ε_3 are the dielectric functions for the Au core, Ag nanoshell, and embedding regions respectively, c denotes the semimajor axis and $a=b$ the semiminor axis. t_T denotes the Ag shell thickness in transverse direction and t_L denotes the Ag shell thickness in longitudinal direction

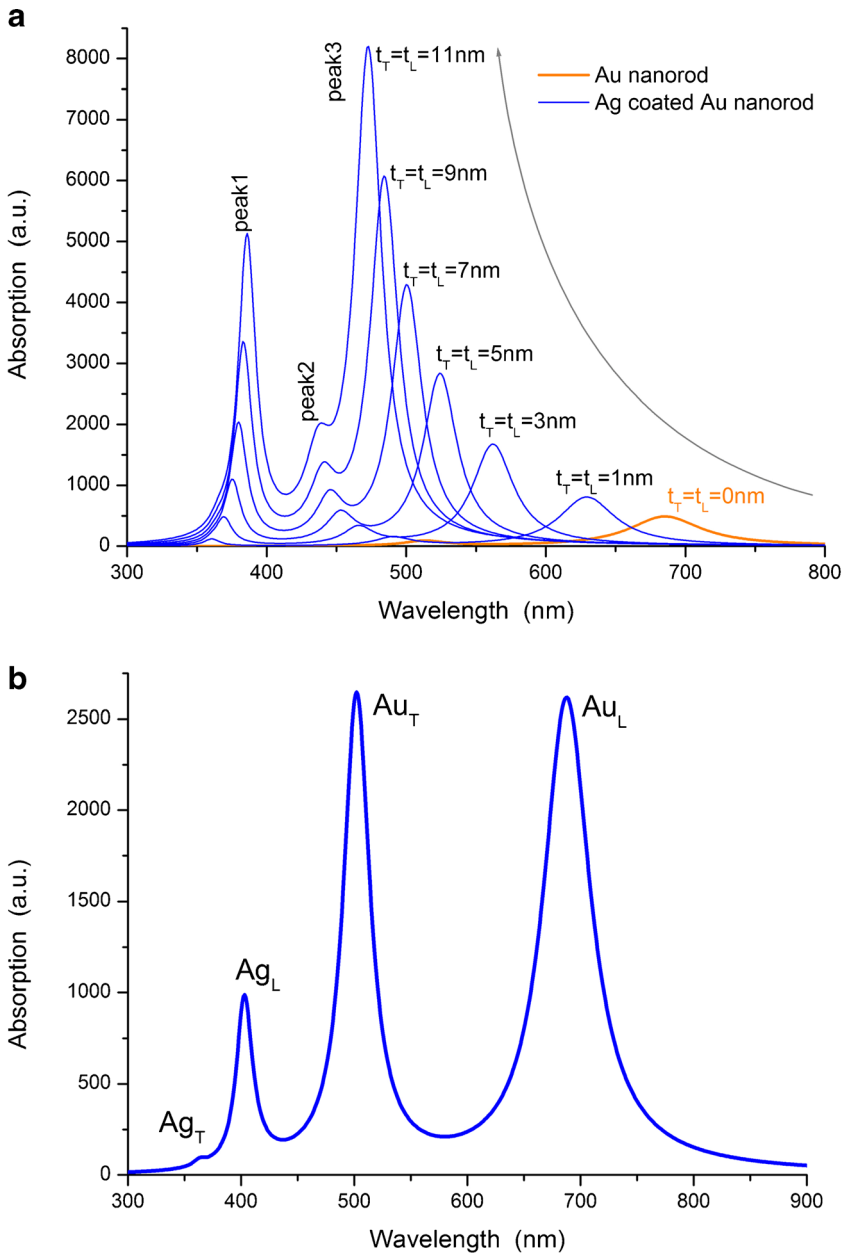

Fig. 2 **a** Calculated absorption spectra of Au–Ag core–shell nanorods with homogeneous Ag coating, the Ag shell thickness is changed from 0 to 11 nm. **b** Calculated absorption spectrum of Au–Ag core–shell nanorods with nonhomogeneous Ag coating, t_T=7.5 nm and t_L=3.25 nm

experimental results [21]. Because the Ag nanoparticles have more intense plasmonic absorption, the physical mechanism of the intensity increasing of peaks 2 and 3 could be resulted from the increase composition of Ag in the Au–Ag bimetallic nanoparticles [21]. Because the Ag nanoparticles have shorter plasmon resonance wavelength, the intense blue shift of peaks 2 and 3 should also be attributed to the increase composition of Ag in the bimetallic nanoparticles. On the other hand, a homogeneous Ag layer coating lowers the overall aspect ratio of the core–shell nanostructure, which provides the minor reason of the blue shift of peak 3.

Although the surface plasmons are coherent excitation and are affected by the coupling between metallic surfaces, different surface electron oscillations may take major effect on different plasmon modes. In our previous study of the transverse LSPR in Au–Ag and Ag–Au core–shell structure nanowires, the two plasmonic peaks have been assigned to outer surface of wall metal and the interface between core and wall metals, respectively [19]. Therefore, there should be four LSPR peaks in the Au–Ag core–shell nanorod. However, one could only find three distinct plasmon peaks in Fig. 2a. The peaks 2 and 3 correspond to the transverse and longitudinal plasmon from Au–Ag interface (denoted as Au_T and Au_L). The peak 1 corresponds to the longitudinal plasmon from outer Ag surface (denoted as Ag_L). Because the transverse plasmonic absorption is always weaker than the longitudinal mode, the fourth peak corresponding to the transverse plasmon from outer Ag surface (denoted as Ag_T) is usually too weak to be observed and could only be found under certain conditions. For example, when the Ag coating is nonhomogeneous (t_T=7.5 nm and t_L=3.25 nm) and the environmental dielectric constant is increased to 3.5, one can find four LSPR peaks in the absorption spectrum as shown in Fig. 2b. In the absorption spectral testing, the gold nanorods are usually suspended in the aqueous solution with a surrounding dielectric constant of $\varepsilon_{\text{surrounding}}$=1.7. Thus, it has been observed that the longitudinal absorption intensity is usually larger than the transverse intensity. In Fig. 2a, the surrounding dielectric constant is set as ε_3=1.0, and the longitudinal absorption intensity is also larger than the transverse intensity. However, when the surrounding dielectric constant is increased, the polarization of the dielectric media will affect the surface plasmon resonance. Because of the nonspherical symmetry, the effect on the transverse and longitudinal SPR is different. Previous experimental reports indicate that the transverse absorption increases and the longitudinal decreases when the surrounding dielectric constant is increased [24–26]. For example, by comparing the absorption spectra of bare Au nanorods and silica-coated Au nanorods, one can find that the transverse absorption increases and the longitudinal decreases as the silica coat thickness increased [24]. In Fig. 2b, in order to observe the fourth peak corresponding to the transverse plasmon from outer Ag surface, the surrounding dielectric constant is increased to ε_3=3.5. Therefore, the transverse plasmon absorption from Au–Ag interface increases greatly, whereas the longitudinal plasmon absorption from Au–Ag interface fades down.

Absorption spectra of Au–Ag nanorods with nonhomogeneous silver coating

In Fig. 3, we studied the effect of nonhomogeneous Ag coating on the absorption spectral properties of Au–Ag core–shell nanorods. For the case of $t_T=2t_L$, i.e., the Ag shell coating in the transverse direction is faster than that of longitudinal direction, the overall aspect ratio decreases rapidly and the composition of Ag in the bimetallic particle increases rapidly. Therefore, the peak 3 blue shifts intensely and the peak 1 gets intense rapidly as the Ag shell thickness is increased. As shown in Fig. 3a, the intensity increase of peak 1 is faster than that of peak 3, which is similar to the experimental observation [3]. Thus, the peak 1 at shorter wavelength becomes more intense than the peak 3 at longer wavelength when the Ag coating is thick, which is different from the calculation results of homogeneous coating case in Fig. 2a and the experimental result of [21]. Furthermore, because of this nonhomogeneous silver coating, the bimetallic nanostructures could present two intense plasmonic absorption peaks with equal intensity and small wavelength gap ca. 30 nm as the Ag shell thickness has a critical value, as shown in the inset of Fig. 3a. This plasmonic property provides potential for double-channel optical sensing based on plasmonic absorption [27]. In Fig. 3a, the disappearance of peak 2 in absorption spectrum is due to the following reasons. Firstly, the increase of outer Ag shell thickness leads to the great enhancement of peaks 1 and 3, which masks the weak transverse plasmon resonance of inner Au core. This trend could be clearly reflected in Fig. 2a. Secondly, the red shift of peak 1 and blue shift of peak 3 make the peak 2 merged together with peaks 1 and 3. Meanwhile, peak 2 only becomes distinct as the surrounding dielectric constant is large as shown in Fig. 2b. However, the surrounding dielectric constant in Fig. 3a is set as ε_3=1, which is much smaller than that of Fig. 2b. Therefore, the peak 2 in Fig. 3a is too weak to be observed.

In order to make the Ag coating-dependent intensity changing clearer, we also plotted the peak intensity of the absorption as the function of Ag coating thickness in Fig. 3c. When $t_T=2t_L$, the intensity of peak 3 is always a little greater than that of peak 1 as the Ag shell thickness is less than 8 nm. The increasing speed of peak 3 fades down as the Ag coating is further increased. And then peaks 3 and 1 have the same intensity when Ag shell thickness reaches 9 nm. However, the intensity difference between peaks 1 and 3 increases again when the Ag shell thickness is greater than 9 nm. For the case of $t_L=2t_T$, i.e., the Ag shell coating in the longitudinal direction is faster than that of transverse direction (but the ratio t_L/

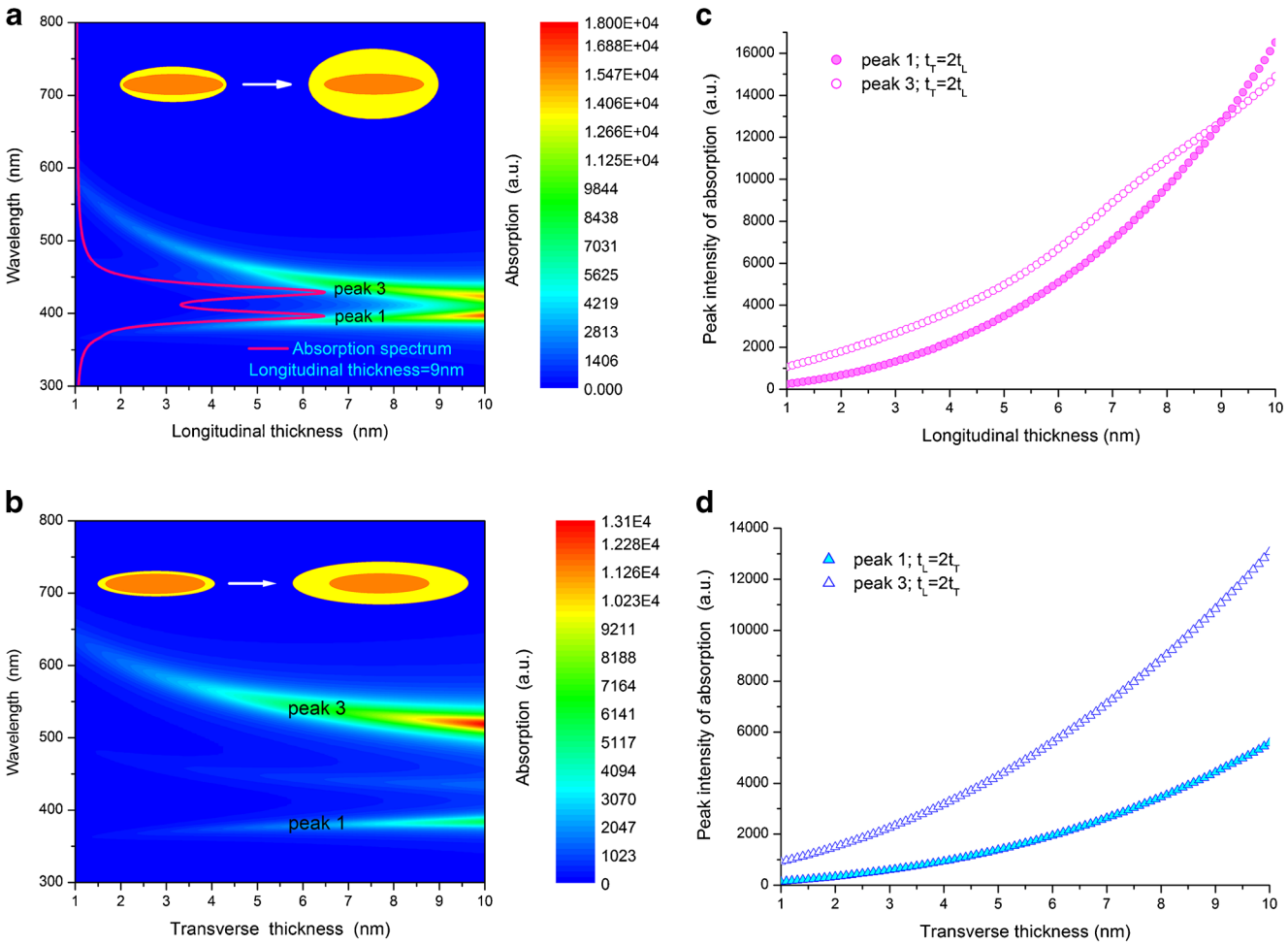

Fig. 3 Calculated absorption spectra of Au–Ag core–shell nanorods with nonhomogeneous silver coating, the Au nanorod core has a large aspect ratio of $p=4$. **a** Transverse Ag shell thickness is larger, $t_T=2t_L$. **b** Longitudinal Ag shell thickness is larger, $t_L=2t_T$. **c** Peak intensity of the absorption as a function of longitudinal Ag coating thickness. **d** Peak intensity of the absorption as a function of transverse Ag coating thickness, $\varepsilon_3=1.0$

$t_T<p$), the overall aspect ratio decreases slowly and the Ag composition of the bimetallic particle also increases slowly. Therefore, the blue shift of peak 3 is gentle and the wavelength gap between peaks 1 and 3 is wide as shown in Fig. 3b. Furthermore, the intensity increase of peak 1 is also gentle and is always weaker than peak 3. As shown in Fig. 3c, d, the intensity difference between peaks 1 and 3 has been monotonously enlarged as the Ag coating is increased. And we cannot obtain two intense plasmonic absorption peaks with equal intensity when the longitudinal Ag coating is thicker as shown in Fig. 3d.

In order to find the effect of aspect ratio of the Au nanorod on the nonhomogeneous coating-dependent plasmonic absorption, we also plotted the absorption spectra of Au–Ag core–shell nanorods when the aspect ratio of the Au nanorod core is decreased to $p=2$. As shown in Fig. 4, the way of the absorption intensity changing and wavelength shifting is similar to the cases of $p=4$. However, because of the decrease of the aspect ratio and the volume of the Au nanorod, the Ag coating-dependent Ag composition increase becomes intense. Therefore, the Ag coating-induced absorption intensity increase becomes rapid. Thus, we can obtain two intense plasmonic absorption peaks with equal intensity and small wavelength gap when the Ag coating thickness is thin. As shown in the inset of Fig. 4a, the Au–Ag core–shell nanorods present two intense plasmonic absorption peaks with equal intensity and small wavelength gap ca. 45 nm as the longitudinal Ag shell thickness is 4 nm. The peak intensity of the absorption as the function of longitudinal Ag coating thickness has been plotted in Fig. 4c. When $t_T=2t_L$, the intensity of peak 3 is always greater than that of peak 1 as the Ag shell thickness is less than 4 nm. However, the increasing speed of peak 3 gets intense first and then fades down as the Ag coating is increased. At last, peaks 3 and 1 have the same intensity when Ag shell thickness reaches 4 nm. In Fig. 4b, because the intensity discrepancy between transverse and longitudinal plasmonic absorption is decreased, the relative intensity of peak 2 is much greater than that of the absorption spectra in

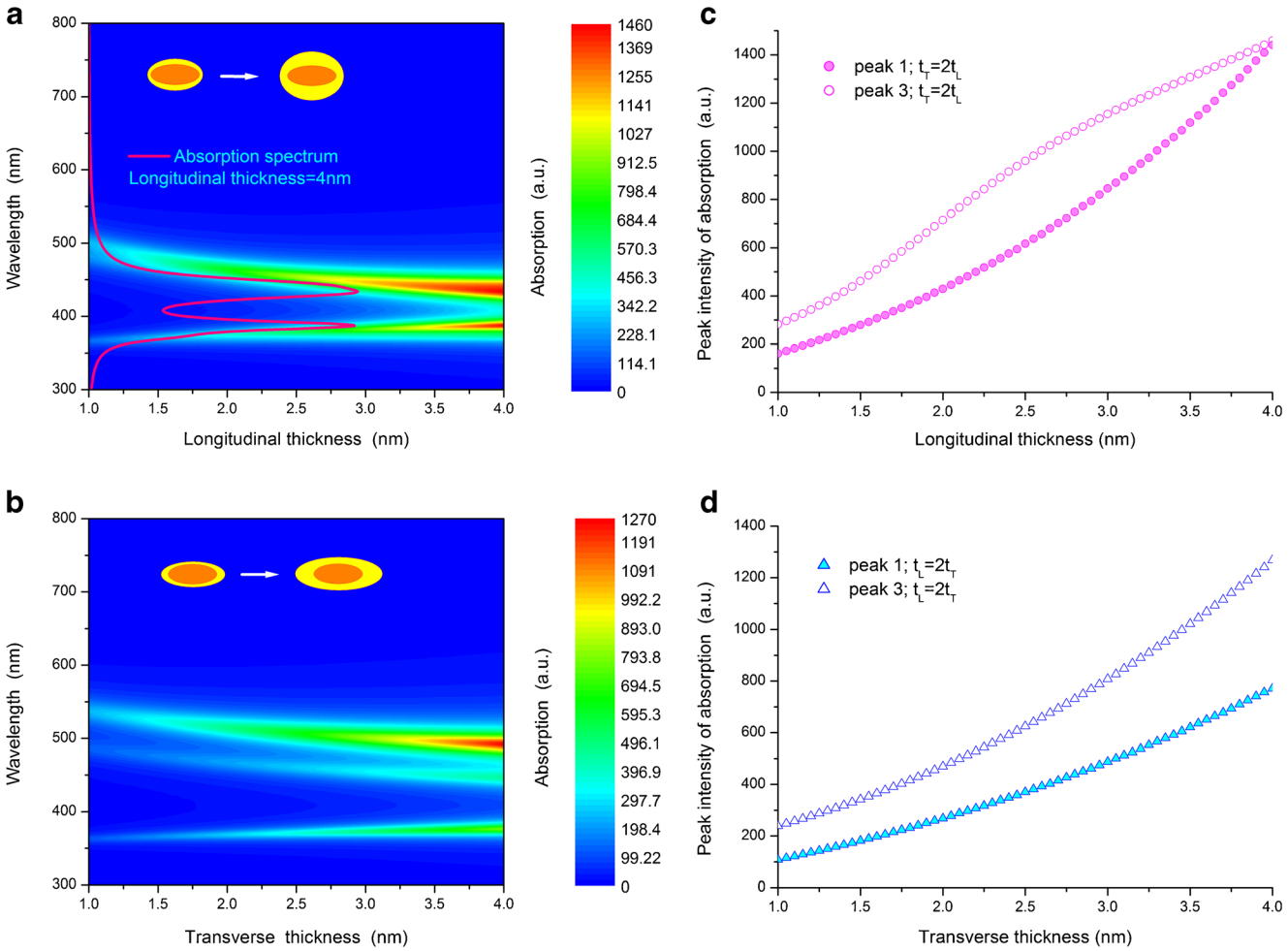

Fig. 4 Calculated absorption spectra of Au–Ag core–shell nanorods with nonhomogeneous silver coating, the Au nanorod core has a small aspect ratio of $p=2$. **a** Transverse Ag shell thickness is larger, $t_T=2t_L$. **b** Longitudinal Ag shell thickness is larger, $t_L=2t_T$. **c** Peak intensity of the absorption as a function of longitudinal Ag coating thickness. **d** Peak intensity of the absorption as a function of transverse Ag coating thickness, $\varepsilon_3=1.0$

Fig. 3b. We can always find three distinct absorption peaks as the Au nanorod is short and the longitudinal Ag coating is thicker.

Experimental study of the absorption spectra of Au–Ag nanorods with silver coating (transverse coating is larger than longitudinal coating)

The preparation of Au nanorods

Au nanorods were prepared according to a seed-mediated growth protocol developed by Sau and Murphy with some slight modification [28]. Initially, Au seed solution was prepared by quickly injecting $NaBH_4$ (0.01 M, 0.6 mL) into the mixture of $HAuCl_4$ (0.01 M,0.25 mL) and CTAB (0.1 M, 7.5 mL) solution in a test tube of 15 mL, followed by 1 min of violent stirring. The color of the solution changed from yellow to brownish yellow, which indicates the start formation of the Au seed. Then, the resultant solution was kept at 27 °C for 2 h for the next use. Secondly, to grow Au nanorods, 0.01 M $HAuCl_4$ (4 mL), 0.01 M $AgNO_3$, 0.1 M AA (0.64 mL), and 1 M HCl were injected into 0.1 M CTAB (90 mL) in order. With gentle stirring, the color of the solution changed from brownish yellow to transparent. Different aspect ratios of gold nanorods could be obtained by tuning the volume of $AgNO_3$ and HCl. Finally, 0.2 mL Au seed solution was injected to initiate growth reaction. Then the ultimate solution was kept at a constant temperature of 27 °C undisturbed overnight. During this time, the transparent solution progressively changed to purple or deep blue, depending on the aspect ratio of the Au nanorods. When the volume of $AgNO_3$ is relatively small, we obtained the shorter Au nanorods with an aspect ratio of 3.3. Figure 5a depicted the synthesized shorter Au nanorods with an average length of about 40 nm and width of about 12 nm. In order to get longer Au nanorods, the $AgNO_3$ volume has been increased and HCl was added at the same time. As shown in Fig. 5b, longer Au nanorods with an aspect ratio

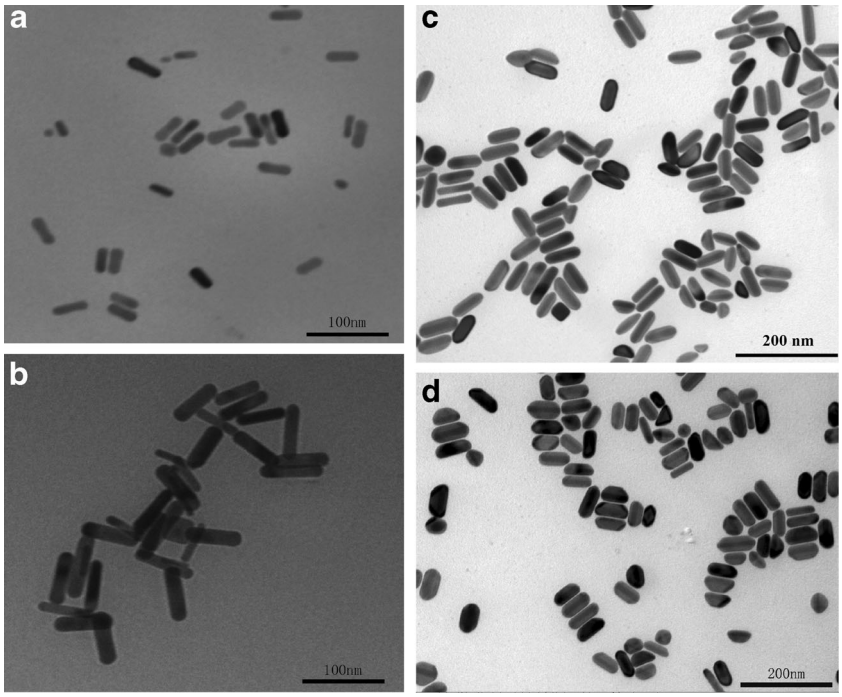

Fig. 5 TEM images of **a** short Au nanorods with an aspect ratio of 3.3. **b** Long Au nanorods with an aspect ratio of 4.8. **c** Au–Ag core–shell nanorod with thin Ag shell thickness. **d** Au–Ag core–shell nanorod with thick Ag shell thickness

of 4.8 (with an average length of about 62 nm and width of about 13 nm) were obtained.

The synthesis of Au–Ag core–shell nanorods

Au nanorods with Ag coating were prepared by the method in previous literature with some minor modification [3, 16, 29, 30]. In summary, 45 mL prepared Au nanorods were centrifuged for 20 min at 10,000 rpm, then the supernatant was carefully removed and the precipitate was redispersed into the same volume of 0.08 M CTAB. One minute of the ultrasonic solution is needed. Afterwards, the solution is divided into nine portions. For each portion, $AgNO_3$ (0.01 M), AA (0.1 M, 0.4 mL), and NaOH (0.1 M, 1 mL) was added in that order. By adding the volume of $AgNO_3$ from 0.1 to 0.9 mL, we obtained Au–Ag core–shell nanorods with different Ag shell thickness. The solution was then kept at 65 °C for 4 h. The typical TEM images of the synthesized Au–Ag core–shell nanorods with thin Ag coating and thick Ag coating are compared. As can be observed in Fig. 5c, when the volume of $AgNO_3$ is 0.5 mL, the Ag shell at the side facet is thin, whose average thickness is about 5 nm. And thicker Ag shell at the side facet of about 10 nm could be observed when the volume of $AgNO_3$ reaches 0.8 mL as shown in Fig. 5d.

Figure 6a depicts the absorption spectra of Au–Ag core–shell nanorods with longer Au nanorods core. As can be seen in Fig. 6a, for longer gold nanorods, as the volume of $AgNO_3$ is increased, peak 1 slightly red shifts with intensity increasing quickly, while peak 3 blue shifts greatly with intensity increasing slowly. At the same time, peak 2 attenuated and then disappeared. The intensity difference between peaks 1 and 3 becomes smaller and smaller with the continuous increase of $AgNO_3$. We can obtain two intense plasmonic absorption peaks with equal intensity when the volume of $AgNO_3$ reaches 0.85 mL, as shown in Fig. 6a. For shorter gold nanorods, two intense plasmonic absorption peaks with equal intensity appeared when the volume of $AgNO_3$ reaches 0.4 mL as shown in Fig. 6b. As the volume of $AgNO_3$ is further increased, peak 1 exceeds peak 3 and leaves only one peak at about 450 nm at last. As a matter of fact, longer and shorter gold nanorods represent aspect ratios of large and small, the volume of $AgNO_3$ corresponds to the thickness of silver coating. The silver coating gets thicker as the amount of $AgNO_3$ is increased. A thin silver layer was developed at first, as shown in line A of Fig. 6b. Owing to its nonhomogeneous coating, the increase of the side of the nanorod's thickness is faster than the end as shown in line B of Fig. 6b. It is obvious that its side facet of silver coating is thicker than line A of Fig. 6b. At last, the nanorods turned to nearly spherical structure as shown in line C of Fig. 6b. Figure 6c, d depicts the dependences of the plasmon peak wavelengths and absorption intensities on the volume of the $AgNO_3$ solution. Because the Ag shell thickness is controlled by the amount of $AgNO_3$, the amount of $AgNO_3$ corresponds to the Ag shell thickness, and the Ag shell thickness is increased as the volume of the $AgNO_3$ solution is increased. Increasing the silver coating results in the

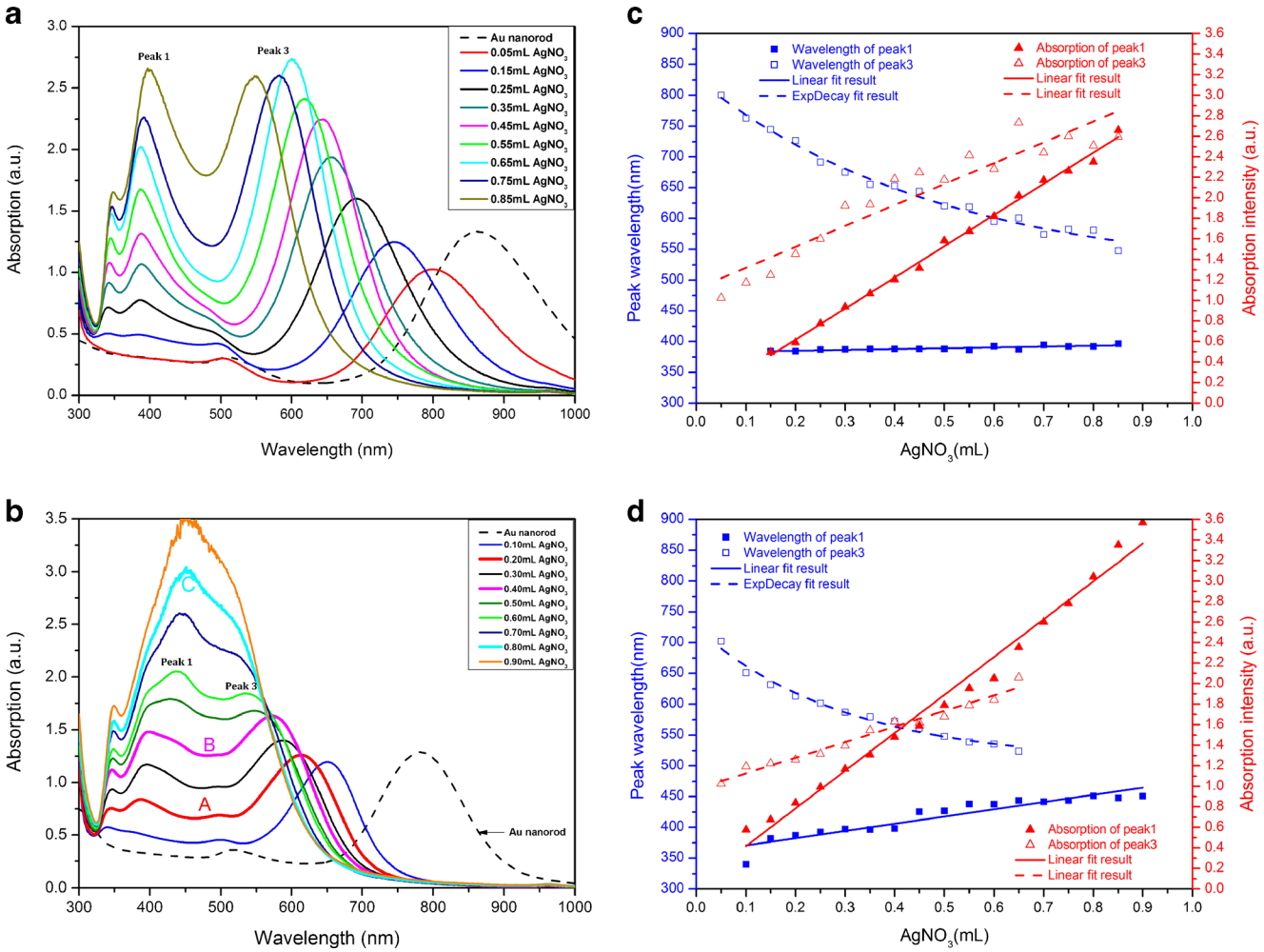

Fig. 6 Absorption spectra of Au nanorod samples and Au–Ag core–shell nanorod samples with different volume of the 0.01 M $AgNO_3$ solution. **a** The Au nanorods have large aspect ratio and the $AgNO_3$ volume is increased from 0.05 to 0.85 mL with an increment of 0.1 mL. **b** The Au nanorods have small aspect ratio and the $AgNO_3$ volume is increased from 0.1 to 0.9 mL with an increment of 0.1 mL. Dependences of the plasmon peak wavelengths and absorption intensities on the volume of the $AgNO_3$ solution, the Au nanorods have a **c** large aspect ratio and **d** small aspect ratio

absorption intensity of both peaks 1 and 3, getting intense linearly. The linear relation could also be found for the silver coating-dependent plasmon shifting of peak 1. However, the peak 3 blue shift exponentially as the silver coating is increased. Furthermore, one can find the silver coating-dependent intensity increasing of peak 1 is more intense as the gold nanorods are short. Therefore, two absorption peaks with equal intensity could be obtained with thinner silver coating. These experimental observations are in good agreement with our theoretical calculation above.

Conclusions

In conclusion, nonhomogeneous Ag coating of the Au nanorod and aspect ratio of Au nanorod core strongly affect the intensity change and wavelength shift of the plasmonic absorption. Theoretical calculations show that, when the transverse Ag coating is faster, the Au–Ag core–shell nanorod could present two intense longitudinal plasmonic absorption peaks with equal intensity and small wavelength gap as the Ag shell thickness has a critical value. When the longitudinal Ag coating is faster, the intensity increasing of longitudinal peak corresponding to outer Ag surface is always weaker than the longitudinal peak corresponding to Au–Ag interface. The critical value of Ag shell thickness could be decreased when Au nanorod is short, at the same time the transverse peak corresponding to Au–Ag interface could be enhanced. It is worth noting that the two equal intensity of absorption peaks exhibit Au–Ag core–shell nanorod obtained from the nonhomogeneous silver coating may have great potential for many biological and chemical applications such as design and fabrication of dual-channel SPR sensor.

Acknowledgments This work was supported by the Program for New Century Excellent Talents in University under grant no. NCET-10-0688, the Fundamental Research Funds for the Central Universities under grant no. 2011jdgz17, and the National Natural Science Foundation of China under grant nos. 11174232, 61178075, and 81101122.

References

1. Moskovits M, Srnová-Šloufová I, Vlčkova B (2002) Bimetallic Ag–Au nanoparticles: extracting meaningful optical constants from the surface-plasmon extinction spectrum. J Chem Phys 116:10435–10446
2. Xu HX (2005) Multilayered metal core–shell nanostructures for inducing a large and tunable local optical field. Phys Rev B 72: 0734051–0734055
3. Jiang R, Chen H, Shao L, Li Q, Wang J (2012) Unraveling the evolution and nature of the plasmons in (Au core)–(Ag shell) nanorods. Adv Mater 24:OP200–OP207
4. Zhang Q, Moran CH, Xia XH, Rycenga M, Li NX, Xia YN (2012) Synthesis of Ag nanobars in the presence of single-crystal seeds and a bromide compound, and their surface-enhanced Raman scattering (SERS) properties. Langmuir 28:9047–9054
5. Li Y, Jing C, Zhang L, Long YT (2012) Resonance scattering particles as biological nanosensors in vitro and in vivo. Chem Soc Rev 41:632–642
6. Wu LP, Li YF, Huang CZ, Zhang Q (2006) Visual detection of Sudan dyes based on the plasmon resonance light scattering signals of silver nanoparticles. Anal Chem 78:5570–5577
7. Tao AR, Habas S, Yang PD (2008) Shape control of colloidal metal nanocrystals. Small 4:310–325
8. Chen HJ, Shao L, Woo KC, Ming T, Lin HQ, Wang JF (2009) Shape-dependent refractive index sensitivities of gold nanocrystals with the same plasmon resonance wavelength. J Phys Chem C 113:17691–17697
9. Cardinal MF, Rodríguez-González B, Alvarez-Puebla RA, Pérez-Juste J, Liz-Marzán LM (2010) Modulation of localized surface plasmons and SERS response in gold dumbbells through silver coating. J Phys Chem C 114:10417–10423
10. Tsuji M, Miyamae N, Lim S, Kimura K, Zhang X, Hikino S, Nishio M (2006) Crystal structures and growth mechanisms of Au@Ag core–shell nanoparticles prepared by the microwave-polyol method. Cryst Growth Des 6:1801–1807
11. Xue C, Millstone JE, Li S, Mirkin CA (2007) Plasmon-driven synthesis of triangular core–shell nanoprisms from gold seeds. Angew Chem Int Ed 46:8436–8439
12. Duan J, Park K, MacCuspie RI, Vaia RA, Pachter R (2009) Optical properties of rodlike metallic nanostructures: insight from theory and experiment. J Phys Chem C 113:15524–15532
13. Tsuji M, Matsuo R, Jiang P, Miyamae N, Ueyama D, Nishio M, Hikino S, Kumagae H, Kamarudin KSN, Tang XL (2008) Shape-dependent evolution of Au@Ag core–shell nanocrystals by PVP-assisted *N*,*N*-dimethylformamide reduction. Cryst Growth Des 8: 2528–2536
14. Gong JX, Zhou F, Li ZY, Tang ZY (2012) Synthesis of Au@Ag core–shell nanocubes containing varying shaped cores and their localized surface plasmon resonances. Langmuir 28:8959–8964
15. Hong SC, Choi YJ, Park SH (2011) Shape control of Ag shell growth on Au nanodisks. Chem Mater 23:5375–5378
16. Ma YY, Li WY, Cho EC, Li ZY, Yu TY, Zeng J, Xie ZX, Xia YN (2010) Au@Ag core–shell nanocubes with finely tuned and well-controlled sizes, shell thicknesses, and optical properties. ACS Nano 4:6725–6734
17. Deng JJ, Du J, Wang Ye TYF, Di JW (2011) Synthesis of ultrathin silver shell on gold core for reducing substrate effect of LSPR sensor. Electrochem Commun 13:1517–1520
18. Lee YH, Chen H, Xu QH, Wang J (2011) Refractive index sensitivities of noble metal nanocrystals: the effects of multipolar plasmon resonances and the metal type. J Phys Chem C 115:7997–8004
19. Zhu J (2009) Surface plasmon resonance from bimetallic interface in Au–Ag core–shell structure nanowires. Nanoscale Res Lett 4:977–981
20. Yu K, You GJ, Polavarapu L, Xu QX (2011) Bimetallic Au/Ag core–shell nanorods studied by ultrafast transient absorption spectroscopy under selective excitation. J Phys Chem C 115:14000–14005
21. Liu MZ, Guyot-Sionnest P (2004) Synthesis and optical characterization of Au/Ag core/shell nanorods. Phys Chem B 108:5882–5888
22. Perenboom JAAJ, Wyder P, Meier F (1981) Electronic properties of small metallic particles. Phys Rep 78:173–292
23. Liu MZ, Guyot-Sionnest P (2006) Preparation and optical properties of silver chalcogenide coated gold nanorods. J Mater Chem 16:3942–3945
24. Yi DK (2011) A study of optothermal and cytotoxic properties of silica coated Au nanorods. Mater Lett 65:2319–2321
25. Huang H, Liu X, Zeng Y, Yu X, Liao B, Yi P, Chu PK (2009) Optical and biological sensing capabilities of Au2S/AuAgS coated gold nanorods. Biomaterials 30:5622–5630
26. Marinakos SM, Chen S, Chilkoti A (2007) Plasmonic detection of a model analyte in serum by a gold nanorod sensor. Anal Chem 79: 5278–5283
27. Chakravadhanula VSK, Elbahri M, Schürmann U, Takele H, Greve H, Zaporojtchenko V, Faupel F (2008) Equal intensity double plasmon resonance of bimetallic quasi-nanocomposites based on sandwich geometry. Nanotechnology 19:225302–225306
28. Sau TK, Murphy CJ (2004) Seeded high yield synthesis of short Au nanorods in aqueous solution. Langmuir 20:6414–6120
29. Fu Q, Zhang DG, Yi MF, Wang XX, Chen YK, Wang P, Ming H (2012) Effect of shell thickness on a Au–Ag core–shell nanorods-based plasmonic nano-sensor. J Opt 14:085001–085005
30. Zhu J, Zhang F, Li JJ, Zhao JW (2013) Optimization of the refractive index plasmonic sensing of gold nanorods by non-uniform silver coating. Sensor Actuat B-Chem 183:556–564